

DACA alleviates nerve damage and motor dysfunction via activation on Nrf2 signaling in Parkinson's disease.

Ji Wang¹, Jindong Zhao², Tang Zhou¹, Zhiqi Lin¹, Shuda Yang², Ju Li¹, Rongping Zhang¹, Changan Geng³, Xinglong Chen¹, and Weiyan Hu²

¹Yunnan University of Traditional Chinese Medicine

²Kunming Medical University

³Chinese Academy of Sciences

March 30, 2024

Abstract

Background and Purpose Parkinson's disease (PD) is the fastest growing neurological disorder. Strong evidence reveals that oxidative stress and mitochondrial dysfunction play critical roles in the pathophysiology of PD. Rosemary contains a large number of abietane diterpenoids with antioxidant power and DACA is a modified product from it. The present study revealed the anti-parkinsonian effects of DACA and its possible mechanisms. **Experimental Approach** The PD model was established by treating mice with MPTP and SH-SY5Y cells and primary neurons with MPP+. western blot and immunofluorescence were used to evaluate the neuroprotective effect of DACA. At the same time, the anxiety-like behavior and motor coordination ability of mice were detected. In addition, reactive oxygen species (ROS) detection, mitochondrial membrane potential detection and western blot were used to detect oxidative stress and mitochondrial related signal changes. **Key Results** DACA improved the motor dysfunction of mouse and inhibited the decrease of tyrosine hydroxylase (TH) positive neurons in substantia nigra (SN) and TH protein expression in midbrain and striatum. It also enhanced the expression of nuclear factor erythroid 2-related factor 2 (Nrf2) and its downstream antioxidant enzymes in midbrain and striatum. DACA prevented MPP+- induced toxicity, reduced oxidative stress and maintained mitochondrial function. The neuroprotective effects of DACA were associated with its ability to induce Nrf2 into nucleus and regulate mitophagy. **Conclusion and Implications** In conclusion, we demonstrated that DACA exerted significant neuroprotection against through the regulation of Nrf2 signaling, suggesting the use of DACA as a possible food supplement in the prevention of PD.

1. Introduction

Parkinson's disease (PD) is the second most prevalent multifactorial progressive neurodegenerative disorder, following Alzheimer's disease, with no currently available curative interventions^[1, 2]. The main pathology of PD is characterized by progressive degeneration of dopamine neurons in the substantia nigra (SN), a significant decrease in striatal dopamine levels, and progressive dysfunction of the body's motor system^[3, 4]. Accumulating evidence from human studies and various experimental models of PD suggests that oxidative stress and mitochondrial dysfunction play pivotal roles in this pathological process^[5-7]. Therefore, targeting reduction of oxidative stress, enhancement of mitochondrial function, and maintenance of autophagy homeostasis help devise strategies to prevent or delay the progression of PD^[8-11].

Nuclear Factor-Erythroid Factor 2 (Nrf2) is an important transcription factor that regulates the expression of large number of genes in healthy and disease states^[12, 13]. Nrf2 regulates oxidative stress, mitochondrial biogenesis, mitochondrial autophagy, autophagy and mitochondrial function in peripheral nervous system and central nervous system^[14, 15]. In response to conditions of oxidative stress, Nrf2 dissociates from Kelch-like ECH-associated protein-1 (Keap1) and translocates into the nucleus, where it binds to antioxidant

response elements (AREs), thereby initiating the transcriptional activation of downstream antioxidant enzymes such as heme oxygenase 1 (HO-1), superoxide dismutase (SOD), glutamate cysteine ligase (GCL), and NAD(P)H quinone oxidoreductase 1 (NQO1)^[16]. The antioxidant enzymes subsequently fulfill an antioxidative function. Recent studies have showed the involvement of Nrf2 in the autophagy pathway^[17]. The activation of Nrf2 triggers autophagy through Sequestosome 1 (SQSTM1, p62), which directly interacts with Keap1 and facilitates its degradation via the autophagic process^[18, 19]. Interestingly, when Nrf2 is largely translocated into the nucleus, it also upregulates the transcription of autophagy-related genes, including p62 and PINK1 (PTEN - induced kinase 1), whose promoters ARE included in the ARE nucleotide sequence, thereby forming a p62 - Keap1 - Nrf2 positive feedback loop^[20]. (Fig. 1)

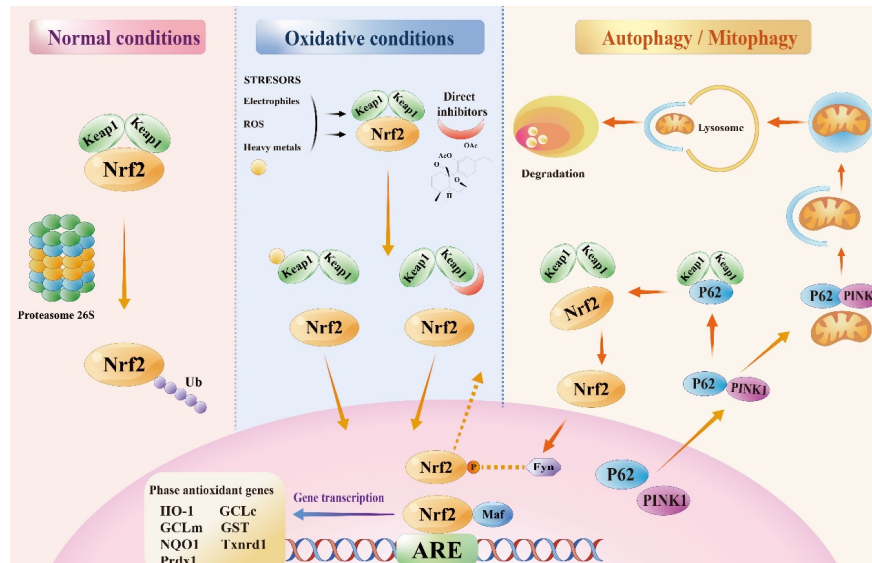


Fig. 1. The regulatory mechanism of Nrf2. Under normal circumstances, Nrf2 is inhibited by Keap1 in the cytoplasm. In the presence of oxidative stress, Nrf2 is transferred to the nucleus to trigger the expression of downstream antioxidant genes. Nrf2 also regulates mitochondrial autophagy and is regulated by it. DACA is identified as an activator of Nrf2 by inhibiting Keap1, which provides a promising target against PD.

Rosmarinus officinalis L. (rosemary) is one of the most popular perennial culinary herbs cultivated all over the world^[21]. Both fresh and dried leaves of rosemary have been used in food cooking or consumed in small amount as herbal tea. Rosemary extracts are routinely employed as natural antioxidant to improve the shelf life of perishable foods^[22-24]. Our team has been engaged in the research and evaluation of phytochemicals for many years, and found that rosemary is rich in diterpenoids^[25, 26]. DACA is the product of structural modification of one of diterpenoids with antioxidant activity and neuroprotective effect. But its therapeutic potential in PD has not been elucidated. The objective of the current study is to explore the protective effects of DACA in animal and cell models of PD and to investigate mechanism of its neuroprotection.

2. Materials and methods

2.1 Chemicals and reagents

Antibodies against HO-1 (ab68477), GCLC (ab190685), GCLM (ab126704), p62 (ab109012), Pink1 (ab216144), Bax (ab32503), Bcl-2 (ab194583), TH (ab137869), PCNA (ab92552), β -actin (ab8226), Tuj1 (ab18207), anti-rabbit (ab6721) and anti-mouse (ab6789) were purchased from abcam (USA). Antibodies against Nrf2 (16396-1-AP) and LC3 (81004-1-RR) were purchased from proteintech (Wuhan, China). GSH/GSSG ratio detection assay kit (ab205811) and reactive oxygen species assay kit (ab113851) were bought from abcam (USA). RIPA buffer (89900), protease and phosphatase inhibitors (78442), nuclear and

total protein extraction (78833), Bicinchoninic acid (BCA) protein assay kit (23225), the enhanced chemiluminescence reagents (34580), the MitoSOX red mitochondrial superoxide indicators (M36008), bovine serum albumin (BSA) (37520), Alexa Fluor 488(A11001) and Alexa Fluor 546(A10040) were purchased from Thermo Scientific (USA). 1-methyl-4-phenylpyridine iodide (MPP⁺) (D048), 1-methyl-4-phenyl-1,2,3,6-tetrahydropyridine (MPTP) (M0896), and poly-D-lysine hydrobromide (P6407) were bought from Sigma Aldrich (Shanghai, China). The cell counting kit-8 (CCK-8) assay kit (4483230) was bought from Adamas Life (Shanghai, China). Total SOD activity detection kit (S0101S) was purchased from Beyotime Biotechnology (Shanghai, China). JC-1 staining reagent (D22200-1) was purchased Bridgen (Beijing, China). 4, 6-2-2-phenyl indole (DAPI) (S2110) was bought from Solarbio (Beijing, China). Trypsin (15050065) and neurobasal medium (12348017) were purchased from Gibco. (USA). Dulbecco's Modified Eagle Medium/Nutrient Mixture F12 Ham (DMEM/F12) (C3130-0500), fetal bovine serum (FBS) (C04001), and penicillin and streptomycin (P/S) mixture (C3420-0100) were purchased from VivaCell (Shanghai, China). For information on DACA, refer to supplementary material. All the other chemicals used were of analytical grade.

2.2 Animals and drug treatment

Pregnant C57BL/6 mice at 16–18 days gestation and adult male C57BL/6 mice were purchased from Department of Laboratory Animal Science, Kunming Medical University. All the animal-related operations were strictly in compliance with the relevant laws and regulations on the use and care of laboratory animals in China. The animal experiment part of this project was approved by the animal ethics committee of Kunming Medical University of Technology, and experiment was conducted as per the Guide for the Care and Use of Laboratory Animals at the Kunming Medical University, Kunming, China. Animals were raised in an environment temperature of 22 ± 2 , 60% humidity and 12-hour light/dark cycle, with available food and water. PD models were prepared using intraperitoneal injection of MPTP. After 1 week of acclimatization under standard conditions, animals were divided into 5 groups (n=13). Group I, normal control, saline (i. p.); Group II MPTP (30 mg/kg, i. p.); Group III, MPTP treatment (30 mg/kg, i. p.) + DACA (20 mg/kg, i. g.); Group IV, MPTP treatment (30 mg/kg, i. p.) + DACA (40 mg/kg, i. g.); Group V, MPTP treatment (30 mg/kg, i. p.) + DACA (80 mg/kg, i. g.). The trial lasted 7 days.

2.3 Behavioral experiments

The effects of MPTP and DACA drug treatment on motor symptoms in mice were assessed using the pole test and the open field test, both conducted by the same operator. The baseline behavioral measurements of mice were recorded one day prior to the experiment. Behavioral assessments were performed one day after completion of the entire treatment regimen to evaluate the changes in behavior.

(1) Pole test: The experimental apparatus for the mice climbing pole consisted of a sturdy base, an elongated vertical pole measuring approximately 80 cm in length and 1 cm in diameter, and a spherical object. The mice were positioned with their heads facing up on the spherical object at the pinnacle of the pole. Timing commenced upon release of the animal by the experimenter and concluded when one hind-limb made contact with the floor. Three trials were conducted, and subsequently, an average score was calculated.

(2) Open field test(OFT) :The mice open field reaction box was 50cm x 50 cm x 50 cm with black inner wall, and the bottom surface was divided into 16 small squares of 12.5 cm x 12.5 cm. Animals were tested within the first 2–4 h of the dark cycle after being habituated to the testing room for 15 min. Videos were analyzed for the following parameters: time spent moving, distance traveled, number of times the central box is encroached (center entries), time spent in central box (center time), and time spent in corner box (corner time).

2.4 Primary neuron culture

The skull, blood, and meninges were carefully removed from the fetal mice brain. After cortical tissue was digested with 0.125% trypsin for 12min at 37degC, the cell suspension was passed through a filter with 40 μ m mesh size after termination of digestion and then centrifuged at 1000 rpm for 5min. The pellet was then resuspended in neurobasal medium. The cells were distributed on poly-D-lysine hydrobromide coated plates

and half of the neural basal matrix was renewed every 2 days. After 7 to 8 days of culture, neurons were subjected to in vitro experiments.

2.5 Cell culture and drug treatment

The human neuroblastoma SH-SY5Y cell line was purchased from Procell Life Science and Technology and were maintained with DMEM/F12 medium with 10% FBS, 100 U/ml penicillin, and 100 µg/ml streptomycin in a humidified incubator with 5% CO₂ at 37°C. We changed the culture medium every two days and subcultured the cells when the density reached 80%. To investigate the protective effect of DACA on MPP⁺-treated SH-SY5Y cells and primary neuronal cells, we treated cells with PBS, MPP⁺, or DACA + MPP⁺ for 24 h. The concentrations of DACA were 5, 10, and 20 µM and the concentrations of MPP⁺ is 1mM.

2.6 Cell viability

The cell viability was assessed using the CCK-8 assay, following the manufacturer's instructions. 1×10^4 SH-SY5Y cells per well or primary neuronal cells were plated in 96-well plates and incubated for 24 hours. The cells were then treated with different methods and conditions. Then, 100µl of culture medium containing 10mM CCK-8 was added to each well and incubated at 37°C for 2h. Absorbance was measured at 450nm using a microplate reader (HBS-1096B, DeTie, Nanjing, China).

2.7 Intracellular reactive oxygen species (ROS) detection

The procedures of ROS measurement were according to manufacturer's instructions. After drug treatment, cells were incubated in serum-free medium containing 10 µM DCFH-DA for 20 min at 37°C. After three washes with serum-free media, the cells were photographed under an inverted fluorescence microscope and the mean fluorescence intensity was analyzed using the software ImageJ. The fluorescence intensity was also measured with Ex/Em=485/535nm using a multifunctional microplate reader.

2.8 Superoxide dismutase (SOD) activity assay

The intracellular SOD activity was measured with a total SOD activity detection kit, according to the manufacturer's instructions. After drug treatment, the cells were washed once with PBS and collected by centrifugation. The cells were fully lysed in SOD sample preparation solution, and the supernatants were collected at 12,000 x g at 4degC for 5 min. The absorbance was detected at 450 nm and 600 nm (reference wavelength) with a multimode microplate reader, and the SOD activity was calculated.

2.9 GSH/GSSG Ratio Detection Assay

According to manufacturer's instructions, the GSH/GSSG ratio was determined using a GSH/GSSG Ratio Detection Assay Kit. The GSH/GSSG assay use a proprietary non-fluorescent water-soluble dye that becomes strongly fluorescent upon reacting with GSH. Cell samples were prepared after drug treatment, and its signal was read by a fluorescence microplate reader at Ex/Em = 490/520 nm.

2.10 Mitochondrial Superoxide assay

Mitochondrial superoxide level was determined using the MitoSOX Red Mitochondrial Superoxide Indicators according to the protocol provided. Cells were incubated in serum-free medium containing 10 µM red reagent for 20 min at 37°C. After three washes with serum-free media, the cells were photographed under an inverted fluorescence microscope and the mean fluorescence intensity was analyzed using the software ImageJ.

2.11 Mitochondrial membrane potential analysis

Mitochondrial membrane potential was detected by JC-1 staining. Cells were incubated with 10 µg/mL of JC-1 working solution for 20 min at 37 °C in the dark. The maximum excitation wavelength of JC-1 monomer was 514nm, and the maximum emission wavelength was 529nm. The maximum excitation wavelength and emission wavelength of JC-1 polymer were 585nm and 590nm. The images were captured by a fluorescence microscope (ECLIPSE Ts2-FL, Nikon, Japan).

2.12 Western blotting

Brain tissue and cells were placed in RIPA buffer containing protease and phosphatase inhibitors (1%), and residual tissue was removed by sonication and centrifugation (13200rpm, 30 min, 4 °C). The procedure of nuclear and total protein extraction was according to the manufacturer's instructions. Cell/tissue lysates were prepared, and protein concentrations were quantified using the BCA Protein Assay kit. Samples with equal amounts of protein were separated by polyacrylamide gel electrophoresis and transferred to polyvinylidene difluoride membranes blocked in 5% skim milk for 2 h at indoor temperature. Then, the membranes were incubated with primary antibodies against Nrf2 (1:2000), HO-1 (1:5000), GCLC (1:5000), GCLM (1:5000), p62 (1:5000), Pink1 (1:1000), LC3 (1:1000), Bax (1:5000), Bcl-2 (1:1000), TH (1:5000), PCNA (1:5000) or β -actin (1:5000) overnight at 4 °C. The next day, membranes were washed three times with TBST and incubated with HRP-conjugated anti-rabbit (1:5000) or anti-mouse (1:5000) secondary antibodies for 2 hours at room temperature. Blots were visualized using the enhanced chemiluminescence reagents, and images were analyzed using ImageJ software.

2.13 Immunofluorescence (IF) staining

Immunofluorescence staining was performed on brain sections or cells. Mice perfusion using 0.9% NaCl solution and 4% paraformaldehyde (PFA), then remove the brain, with 4% paraformaldehyde fixed up for the night. After gradient dehydration in sucrose solution, brains were embedded and sectioned. The cells were fixed with 4% PFA at room temperature for 20 to 30 minutes. With 5% bovine serum albumin (BSA) (containing 0.25% Triton X - 100) blocking buffer in the closed for 1 hour at room temperature and then incubated with primary antibodies against Nrf2(1:500), TH (1:500) and Tuj1 (1:1000) overnight at 4 °C. The cells or brain tissue section were incubated with corresponding secondary antibodies Alexa Fluor 488(1:500) and/or Alexa Fluor 546(1:500). After the wash three times with PBS, use amino 4, 6-dimethyl-2-phenyl indole (DAPI) redyeing for 5 minutes. Fluorescence was captured on Confocal laser scanning micros (AX | AX R with NSPARC, Nikon, Japan). The ImageJ software was used to measure the inflorescence intensity.

2.14 Statistical analysis

GraphPad Prism 9 Software (San Diego, CA, USA) was used for the

statistical analysis of data. The results were performed by mean \pm SEM. Compared multiple groups of data and used one-way ANOVA followed by Tukey's post hoc test. A two-sided P value was used for all tests, and $p < 0.05$ was considered statistically significant.

3. Results

3.1 Discovery of a small molecule DACA against MPP⁺-induced neuronal cells

The potential protective effects of rosemary diterpenes, namely carnosic acid (CA), carnosol (CS), and rosmarinol (RO), were investigated in SH-SY5Y cells. Our results demonstrated that CS significantly enhanced the viability of MPP⁺-induced SH-SY5Y cells, surpassing CA and RO (Fig. 2B). Consequently, we synthesized a carnosol derivative named DACA through a simple structural modification of carnosol (Fig. 2C-D). Notably, DACA exhibited superior anti- MPP⁺ activity compared to carnosol alone without any apparent cytotoxicity towards cells (Fig. 2E). To further validate the neuroprotective effect of DACA, we used MPP⁺ to stimulate primary neurons to evaluate its impact. Our findings revealed that DACA effectively inhibited MPP⁺-induced injury in primary neurons while exhibiting no influence on primary neuron survival when administered alone (Fig. 2E). Collectively, these findings highlight DACA as a valuable small molecule capable of safeguarding against MPP⁺- induced neuronal cell injury.

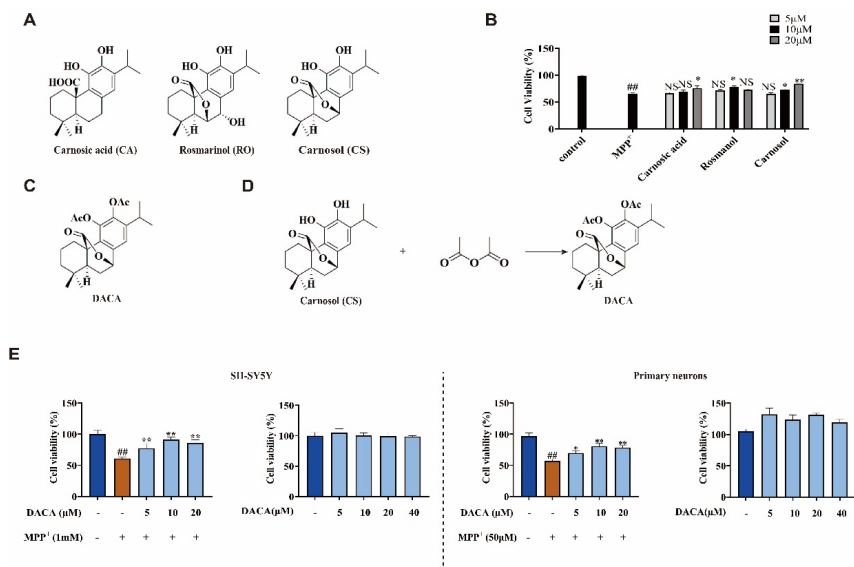


Fig. 2. Discovery of a small molecule DACA against MPP⁺-induced neuronal cells. (A) Chemical structure of Carnosic acid (CA), Rosmarinol (RO), Carnosol (CS). (B) Effects of CA, RO and CS and MPP⁺ on SH-SY5Y cells (n = 5 per group). (C) Chemical structure of DACA. (D) The chemical equation for preparing DACA. (E) Effects of different concentrations of DACA on the viability of SH-SY5Y cells and primary neurons (n = 5 per group). (F) Effects of DACA on the viability of MPP⁺-treated SH-SY5Y cells and primary neurons (n = 5 per group). Data shown are mean ± SEM; #p < 0.05, ##p < 0.01 vs. control; *p < 0.05, **p < 0.01 vs. MPP⁺. NS. not significant.

3.2 DACA alleviates motor dysfunction in MPTP-induced PD mice

The MPTP-induced model serves as a well-established experimental paradigm for investigating molecules associated with Parkinson's disease^[27]. To explore the impact of DACA on motor dysfunction and behavioral changes, we conducted a series of fundamental behavioral experiments, including the open field test and pole climbing test. As depicted in Fig. 3B-C, compared to the control group, MPTP treatment significantly decreased the total distance traveled by mice within the open field box. However, this reduction was ameliorated in all DACA dosage groups. Similarly, MPTP-treated mice exhibited reduced dwell time in the central region and a notable increase in corner time. In contrast, DACA treatment effectively enhanced dwell time in the central region while reducing corner time (Fig. 3B-C). In the climbing pole test, the MPTP-treated group exhibited a significant increase time in falling to the floor and turning head compared with the control group, whereas mice treated with DACA showed a decrease in these parameters (Fig. 3C). These data suggest that DACA mitigates MPTP-induced impairments in muscle control and motor function in mice.

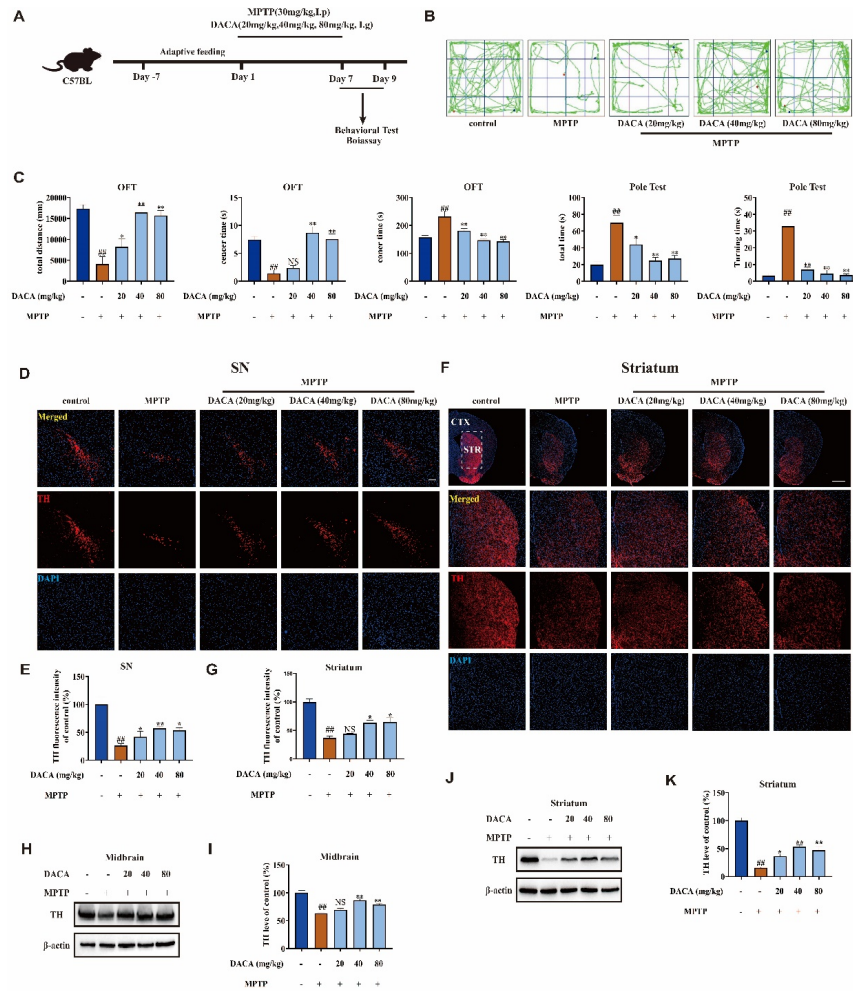


Fig. 3. DACA alleviates motor dysfunction and protects dopamine neurons in mice. (A) Schematic representation of the protocol used for MPTP and DACA treatments. (B-C) Behavior test analysis. Open field test and pole test were recorded and analyzed (n = 12 per group). (D-E) Immunofluorescence analysis of dopamine neurons in brain SN tissue. Scale bar 100 mm. Data are shown as representative pictures (D) and mean fluorescence intensity (E) (n = 5 per group). (F-G) Immunofluorescence analysis of dopamine neurons in striatum tissue. Scale bar 1000 mm. Data are shown as representative pictures (F) and mean fluorescence intensity (G) (n = 5 per group). (H-I) Immunoblot analysis of tyrosine hydroxylase (TH) in midbrain tissue. Data are shown as representative pictures (H) and quantified relative expression (I) (n = 5 per group). (J-K) Immunoblot analysis of tyrosine hydroxylase (TH) in striatum tissue. Data are shown as representative pictures (J) and quantified relative expression (K) (n = 5 per group). Data shown are mean ± SEM; #p < 0.05, ##p < 0.01 vs. control; *p < 0.05, **p < 0.01 vs. MPTP+. NS. not significant.

3.3 DACA protected dopaminergic neurons by preserving the TH level in the substantia nigra(SN) and striatum

The expression of tyrosine hydroxylase (TH), a critical regulator involved in the maintenance and regulation of midbrain neurons, is found to be reduced in patients with PD. Immunofluorescence and Western blot were used to detect the changes of TH levels in the brain of mice to explore the therapeutic effect of DACA.

Immunofluorescence labeling of TH showed that MPTP provokes a marked degeneration of dopaminergic neurons in the SNc and dopaminergic fibers in the Str, which was largely prevented by DACA (Fig. 3D-G). Meanwhile, western blot analysis revealed that DACA significantly attenuate the MPTP-induced decrease of TH levels in the midbrain and striatum (Fig. 3H-K). These results suggest that DACA protects against MPTP-triggered dopamine neurodegeneration in the SN and striatum.

3.4 DACA increased the expression of Nrf2 and its downstream antioxidant enzymes in the midbrain and striatum

Studies conducted over the years have consistently demonstrated that oxidative stress and mitochondrial dysfunction play pivotal roles in the pathological progression of PD. Nrf2 has been identified as an essential antioxidant defense mechanism, safeguarding cells against abnormal levels of ROS. Activation of Nrf2, along with other antioxidant defense systems, is believed to confer protection to dopaminergic cells against MPTP-induced oxidative stress. Consequently, we assessed the impact of DACA on Nrf2 activation in brain homogenates obtained from mice treated with MPTP. Our western blot analysis revealed that MPTP administration led to a reduction in Nrf2 levels within both the striatum (Fig. 4A-B) and midbrain (Fig. 4C-D). Downstream proteins of Nrf2 including HO-1, GCLC, and GCLM exhibited a downward trend. However, following treatment with DACA, the expression levels of these proteins were increased.

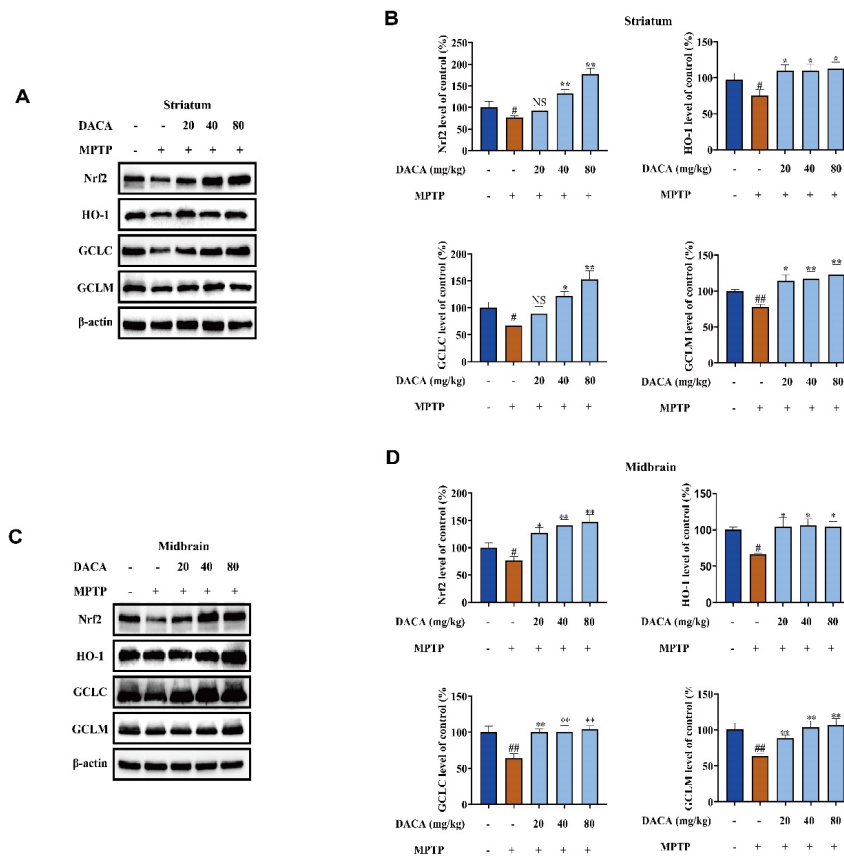


Fig. 4. DACA increases Nrf2 levels in the striatum and midbrain. (A-B) Immunoblot analysis of Nrf2, HO-1, GCLC and GCLM in striatum tissue. Data are shown as representative pictures (A) and quantified relative expression (B) (n = 5 per group). (C-D) Immunoblot analysis of Nrf2, HO-1, GCLC and GCLM in midbrain tissue. Data are shown as representative pictures (C) and quantified relative expression

(D) (n = 5 per group). Data shown are mean \pm SEM; #p < 0.05, ##p < 0.01 vs. control; *p < 0.05, **p < 0.01 vs. MPTP. NS. not significant.

3.5 DACA attenuates oxidative stress by regulating Nrf2 in cells.

We have previously shown that DACA enhances the MPP⁺-induced decrease in cell viability. The measurement of reactive oxygen species (ROS) serves as the most direct evaluation index for detecting oxidative free radicals. A reduction in superoxide dismutase (SOD) activity amplifies the increase in free radicals. When cells are exposed to high levels of oxidative stress, oxidized glutathione (GSSG) accumulates and leads to a decrease in the glutathione (GSH)/GSSG ratio, which has become a valuable tool for assessing cellular damage caused by free radicals and evaluating oxidative stress in cells and tissues. According to the results shown in Fig. 5A-C, it is evident that SH-SY5Y cells and primary neurons treated with MPP⁺ exhibited a significant elevation in ROS levels compared to the control group, accompanied by decreased SOD levels and a reduced GSH/GSSG ratio. However, DACA effectively lowered intracellular ROS levels, prevented SOD dissipation, and increased the GSH/GSSG ratio.

Western blot analysis revealed that treatment with DACA at concentrations of 5 μ M, 10 μ M, and 20 μ M significantly augmented the translocation of Nrf2 to the nucleus and upregulated the expression of its downstream proteins HO-1, GCLC, and GCLM (Fig. 5D-G) in both SH-SY5Y cells and primary neurons. Immunofluorescence staining corroborated the western blot results by demonstrating that DACA facilitated the translocation of cytosolic Nrf2 into the nucleus (Fig. 5H). These findings suggest that activation of Nrf2 leads to an enhancement in cellular antioxidants, which may be responsible for mitigating the toxic effects induced by MPP⁺. Furthermore, immunofluorescence staining using tuji1 demonstrated that MPP⁺ significantly altered neuronal cell morphology, synaptic shortening, and induced round-shaped cells. However, these changes were markedly reversed upon treatment with DACA (Fig. 5H).

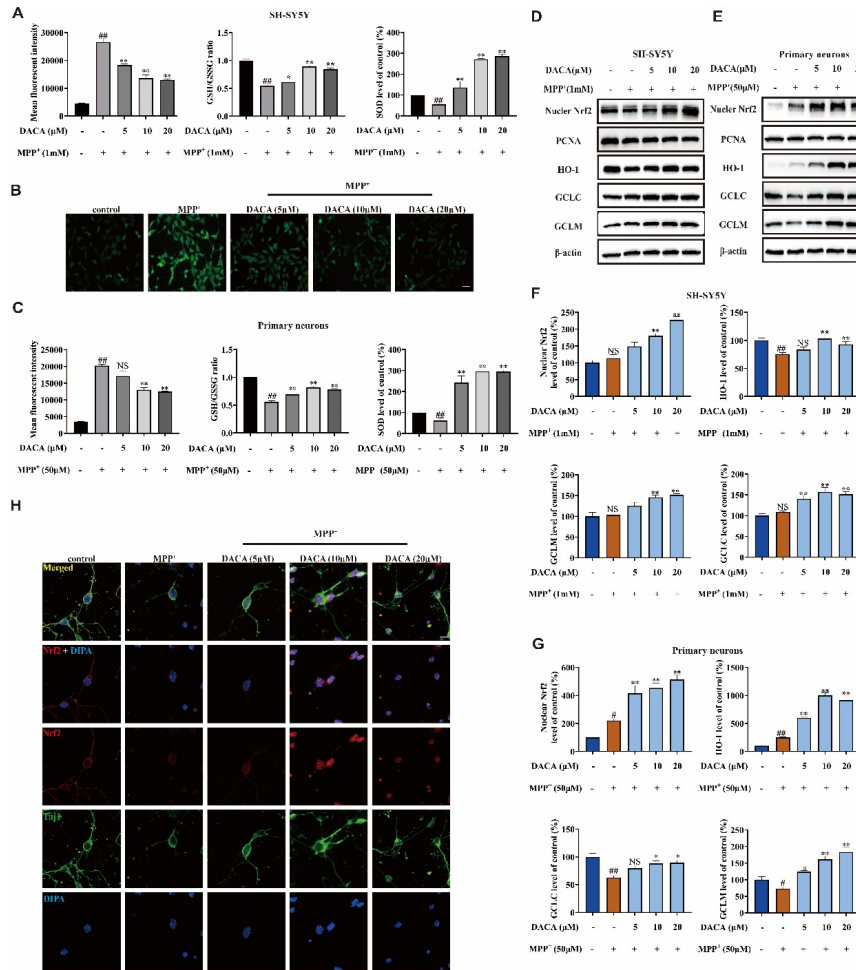


Fig. 5. DACA attenuates oxidative stress by regulating Nrf2 in cells. (A-C) The fluorescence analysis of DCFH-DA and GSH/GSSG in SH-SY5Y cells and primary neurons on a fluorescence plate reader at Ex/Em = 485/535 nm and Ex/Em = 490/520 nm (AC) (n = 5 per group). The analysis of SOD in SH-SY5Y cells and primary neurons is used with ELISA(AC) (n = 5 per group). Representative micrographs of DCFH-DA staining in SH-SY5Y cells (B). Scale bar 100 μm. (D-G) Immunoblot analysis of Nrf2, HO-1, GCLC and GCLM in SH-SY5Y cells and primary neurons. Data are shown as representative pictures (D, E) and quantified relative expression (F, G) (n = 5 per group). (H) Representative image of immunofluorescence staining of Nrf2 in primary neurons. Scale bar 10 μm. Data shown are mean ± SEM (n = 5); *p < 0.05, **p < 0.01 vs. control; #p < 0.05, ##p < 0.01 vs. MPP⁺. NS. not significant.

3.6 The role of DACA in mitochondrial function and autophagy

Mitochondria, a highly adaptable and dynamic organelle, play a crucial role in neuronal apoptosis. We investigated the potential protective effect of DACA on mitochondria. JC-1 staining was employed to assess mitochondrial membrane potential (MMP) in SH-SY5Y cells and primary neurons, mitochondrial superoxide localization was used to evaluate mitochondrial redox potential. Our findings demonstrate that MPP⁺ significantly increased the number of cells with mitochondrial depolarization (green), which was effectively reversed by DACA treatment (Fig. 6A). Furthermore, DACA treatment successfully restored the imbalance in mitochondrial REDOX potential caused by MPP⁺ exposure (Fig. 6B). MPP⁺ induces neuronal cell death through regulation of pro-apoptotic members within the Bcl-2 protein family. To investigate this further, we

performed Western blot analysis to examine changes in Bcl-2 and Bax expression following DACA treatment. The results revealed that DACA counteracted the decrease in Bcl-2 levels and attenuated the increase in Bax induced by MPP⁺, thereby enhancing the ratio of Bcl-2/Bax. These findings suggest that Nrf2 activation mediated by DACA not only preserves mitochondrial health but also prevents cellular apoptosis (Fig. 6E-H).

Mitophagy is a selective cellular process that eliminates senescent, damaged, or redundant mitochondria through autophagy, serving as a crucial pathway for maintaining mitochondrial quality control. Previous studies have demonstrated the regulatory role of Nrf2 activation in autophagy, potentially mediated by p62-Nrf2 interaction. To investigate the impact of DACA on autophagy, we assessed the expression levels of p62, PINK1, and LC3 proteins. Our results (Fig. 6E-H) revealed decreased levels of p62 and PINK1 proteins along with an increased LC3II/LC3I ratio in MPP⁺-treated cells. As hypothesized, DACA activated Nrf2 signaling pathway and subsequently upregulated p62 and PINK1 expression (Fig. 6E-H). Consistently observed in both SH-SY5Y cells and primary neurons, these findings suggest that DACA plays a regulatory role in modulating normal autophagic flux to safeguard cellular homeostasis.

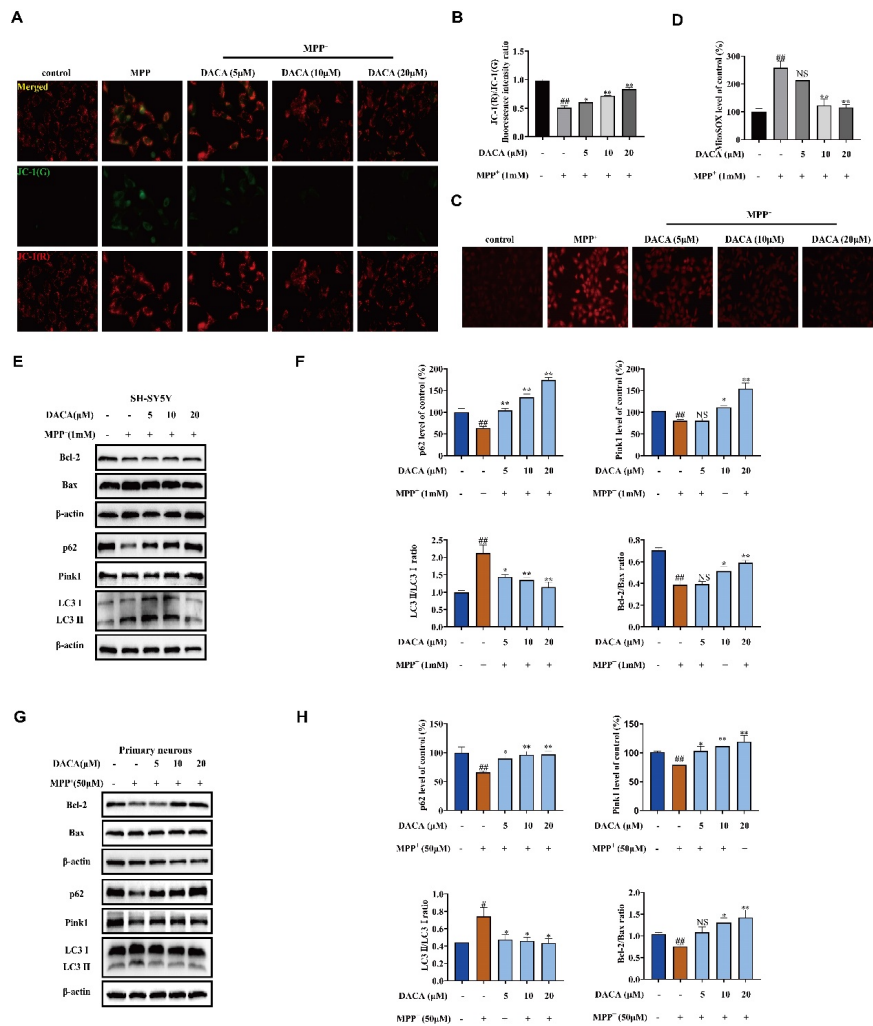


Fig. 6. DACA maintains mitochondrial homeostasis by regulating mitochondrial autophagy. (A-B) Representative micrographs of JC-1 staining in SH-SY5Y cells. Scale bar 100 mm. (B). The fluorescence analysis of JC-1 in SH-SY5Y cells on a fluorescence plate reader at Ex/Em = 514/529 nm and Ex/Em

= 585/590 nm(B) (n = 5 per group). (C-D) Immunofluorescence analysis of mitochondrial superoxide in SH-SY5Y cells. Scale bar 100 nm. Data are shown as representative pictures(C) and mean fluorescence intensity(D) (n = 5 per group). (E-H) Immunoblot analysis of p62, PINK1, LC3, Bax and Bcl-2 in SH-SY5Y cells and primary neurons. Data are shown as representative pictures (E, G) and quantified relative expression (F, H) (n = 5 per group). Data shown are mean ± SEM (n = 5); *p < 0.05, **p < 0.01 vs. control; #p < 0.05, ##p < 0.01 vs. MPP⁺. NS. not significant.

3.7 DACA exerts neuroprotective effects by regulating Nrf2.

We conducted experiments to evaluate the dependence of DACA-induced neuroprotection on Nrf2 activation and the involvement of p62 in the pathway of Nrf2 activation by DACA. ML385, a specific NRF2 inhibitor, and K67, a competitive binder of p62 to Keap1 that restores Keap1-driven degradation of Nrf2 ubiquitination, were employed to investigate the mechanism underlying DACA-mediated Nrf2 expression^[28-30]. The use of Nrf2 inhibitors (ML385) in cell viability tests revealed that the protective effect of DACA against MPP⁺ toxicity was abolished, indicating that Nrf2 activation is essential for DACA's neuroprotective effects. Additionally, in the presence of K67, there was a reduction in the neuroprotective capacity of DACA (Fig. 7A).

To further validate the involvement of DACA in Nrf2 activation, we assessed the intracellular levels of p62, Nrf2, and their downstream proteins. Western blot analysis revealed that ML385 effectively attenuated DACA-induced Nrf2 activation while concurrently reducing the expression of HO-1, GCLC, and GCLM (Fig. 7B-D). Conversely, K67 failed to impede Nrf2 activation (Fig. 7B-D), suggesting that p62 is not a prerequisite for DACA-mediated Nrf2 activation.

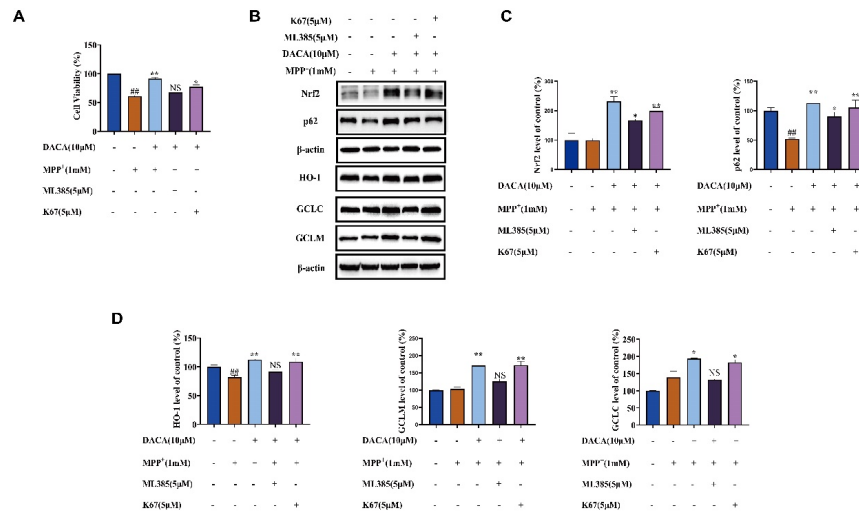


Fig. 7. DACA exerts neuroprotective effects by regulating Nrf2.(A) Effects of K67 and ML385 on DACA treated cell viability (n = 5 per group). (B-D) Immunoblot analysis of Nrf2, p62, HO-1, GCLC and GCLM in SH-SY5Y cells. Data are shown as representative pictures (B) and quantified relative expression (C-D) (n = 5 per group). Data shown are mean ± SEM (n = 5); *p < 0.05, **p < 0.01 vs. control; #p < 0.05, ##p < 0.01 vs. MPP⁺. NS. not significant.

4. Discussion

Rosemary, an herb of economic and gustatory repute, is employed in traditional medicines in many countries^[31]. Rosemary contains CA, CS and abietane-type phenolic diterpenes^[32, 33], which account for most of its biological and pharmacological actions^[34, 35]. In our previous study, we identified DACA as an abietane type diterpene with antioxidant effects. However, no investigations have explored the role of DACA

in PD. The present study demonstrates that: (1) DACA ameliorates MPTP-induced motor dysfunction and decrease of TH level, and induces the upregulation of Nrf2 and its downstream antioxidant enzymes in the midbrain and striatum; (2) DACA alleviate MPP⁺-induced oxidative stress, mitochondrial damage and autophagy abnormalities. (3) The neuroprotective mechanism of DACA operates via the activation of Nrf2.

Parkinson's disease (PD) is a neurodegenerative disorder characterized by resting tremor, bradykinesia, myotonia, postural and gait disturbances as the primary motor manifestations^[36]. The behavioral disorders associated with Parkinson's disease are attributed to the degenerative demise of dopaminergic neurons, and alterations in TH expression exhibit a close correlation with dopaminergic neuronal death^[37, 38]. In this study, DACA treatment effectively mitigated MPTP-induced motor dysfunction and significantly elevated TH levels in the midbrain and striatum. Nrf2 is the master regulator of cellular redox status^[39]. Overexpression of its downstream proteins under neurotoxic conditions prevents hydrogen peroxide accumulation, lipid peroxidation, and, consequently, neuronal loss^[40]. The findings of our study demonstrate that DACA has the potential to enhance the expression levels of Nrf2, HO-1, GCLC, and GCLM in both the midbrain and striatum. This demonstrates that Nrf2 activation using DACA might be able to help brain tissue repair and promote functional recovery.

Accumulating evidence from human studies and various experimental models of PD suggests that oxidative stress plays a pivotal role in both the initiation and progression^[41]. The data obtained from our study demonstrated that DACA exhibited a protective effect against MPP⁺-induced oxidative stress in cells, thereby suggesting its potential as a potent antioxidant compound. The generation of ROS is intricately associated with oxidative stress-induced damage and the pathophysiology underlying neurological dysfunction and neuronal cell death processes. SOD serves as the primary line of defense against free radicals, exhibiting robust and efficient scavenging activity by utilizing free radicals as substrates. GSH, an indispensable antioxidant, effectively mitigates oxidative stress instigated by ROS. Notably, DACA significantly attenuated MPP⁺-induced ROS production and concurrently enhanced the levels of SOD and GSH. Simultaneously, DACA facilitated nuclear translocation of Nrf2 and upregulated the expression of HO-1, GCLC, and GCLM.

Excessive oxidative stress selectively targets and impairs mitochondria, resulting in their functional impairment. The preservation of mitochondrial integrity and bioenergetic functions is crucial for cellular homeostasis^[42]. To maintain mitochondrial and cellular homeostasis while preventing the detrimental effects of damaged mitochondria on cells, a process known as mitophagy occurs wherein cells selectively sequester and degrade dysfunctional or impaired mitochondria^[43, 44]. The results demonstrated that DACA effectively reversed the decline in mitochondrial membrane potential and the elevation of mitochondrial reactive oxygen species induced by MPP⁺. Additionally, DACA exerted regulatory effects on intracellular apoptosis-related proteins Bax and Bcl-2, leading to a significant increase in the Bcl-2/Bax ratio, thereby inhibiting MPP⁺-induced apoptosis. Interestingly, DACA modulated mitophagy through modulation of p62, PINK1, and LC3 expression.

A plethora of studies have demonstrated that Nrf2 not only governs oxidative stress, but also exerts a pivotal role in preserving mitochondrial function and regulating mitophagy^{[41] [45]}. In order to elucidate the localization of Nrf2 in mediating the neuroprotective effects of DACA, we employed a selective inhibitor targeting Nrf2. Intriguingly, treatment with this specific Nrf2 inhibitor abrogated the protective efficacy of DACA against MPP⁺-induced cellular damage. However, with the presence of a specific p62-Nrf2 inhibitor, substantial levels of Nrf2 were still observed within the cellular milieu. This suggests that the neuroprotective effect of DACA is through Nrf2. And unlike most natural small molecules of Nrf2 activators, Nrf2 activation by DACA is not via p62.

4. Conclusion

In summary, the study demonstrates the protective effects of DACA against MPTP-induced motor dysfunction, neurological deficit, and neurodegeneration in a manner consistent. Additionally, DACA exhibits antioxidant properties and plays a crucial role in maintaining mitochondrial health and regulating mitophagy through Nrf2 activation (Fig. 1). These findings significantly contribute to our understanding of the

intricate relationship between Nrf2 and Parkinson's disease (PD). Consequently, DACA holds great promise as a potential anti-PD drug for further therapeutic interventions aimed at preventing PD occurrence and progression. However, it is imperative to conduct future investigations to explore other potential protective effects of DACA as well as its multi-target mechanism of action.

Data Availability

The data that support the findings of this study are available from the corresponding author upon reasonable request.

Conflict of interest

The authors declare that they have no known competing financial interests or personal relationships that could have appeared to influence the work reported in this paper.

Acknowledgment

This work was supported by the Fund of the National Natural Science Program of China (32160107, X. L. C.; 81960666, W. Y. H.), the Joint Program of Yunnan Province and Kunming Medical University (202101AY070001-009, W. Y. H.), Yunnan Province Young Academic and Technical Leaders Project (202105AC160078, W. Y. H.), the Program of Yunling Scholarship (R. P. Z.), the Social Development Special Projects-Key Research and Development Plan of Science and Technology Department of Yunnan Province (202303AC100025, R. P. Z.), and the Open Foundation of Yunnan Key Laboratory of Southern Medicine Utilization (202105AG070012XS23014, J. W.).

References

1. Phukan, B.C., R. Roy, I. Gahatraj, P. Bhattacharya, and A. Borah, Therapeutic considerations of bioactive compounds in Alzheimer's disease and Parkinson's disease: Dissecting the molecular pathways. *Phytother Res*, 2023. 37(12): p. 5657-5699 <https://doi.org/10.1002/ptr.8012>.
2. Heavener, K.S. and E.M. Bradshaw, The aging immune system in Alzheimer's and Parkinson's diseases. *Semin Immunopathol*, 2022. 44(5): p. 649-657 <https://doi.org/10.1007/s00281-022-00944-6>.
3. Kumar, S., L. Goyal, and S. Singh, Tremor and Rigidity in Patients with Parkinson's Disease: Emphasis on Epidemiology, Pathophysiology and Contributing Factors. *CNS Neurol Disord Drug Targets*, 2022. 21(7): p. 596-609 <https://doi.org/10.2174/1871527320666211006142100>.
4. Costa, H.N., A.R. Esteves, N. Empadinhas, and S.M. Cardoso, Parkinson's Disease: A Multisystem Disorder. *Neurosci Bull*, 2023. 39(1): p. 113-124 <https://doi.org/10.1007/s12264-022-00934-6>.
5. Vrijzen, S., M. Houdou, A. Cascalho, J. Eggermont, and P. Vangheluwe, Polyamines in Parkinson's Disease: Balancing Between Neurotoxicity and Neuroprotection. *Annu Rev Biochem*, 2023. 92: p. 435-464 <https://doi.org/10.1146/annurev-biochem-071322-021330>.
6. Moradi Vastegani, S., A. Nasrolahi, S. Ghaderi, R. Belali, M. Rashno, M. Farzaneh, and S.E. Khoshnam, Mitochondrial Dysfunction and Parkinson's Disease: Pathogenesis and Therapeutic Strategies. *Neurochem Res*, 2023. 48(8): p. 2285-2308 <https://doi.org/10.1007/s11064-023-03904-0>.
7. Jomova, K., R. Raptova, S.Y. Alomar, S.H. Alwasel, E. Nepovimova, K. Kuca, and M. Valko, Reactive oxygen species, toxicity, oxidative stress, and antioxidants: chronic diseases and aging. *Arch Toxicol*, 2023. 97(10): p. 2499-2574 <https://doi.org/10.1007/s00204-023-03562-9>.
8. Trist, B.G., D.J. Hare, and K.L. Double, Oxidative stress in the aging substantia nigra and the etiology of Parkinson's disease. *Aging Cell*, 2019. 18(6): p. e13031 <https://doi.org/10.1111/acer.13031>.
9. Hassanzadeh, K. and A. Rahimmi, Oxidative stress and neuroinflammation in the story of Parkinson's disease: Could targeting these pathways write a good ending? *J Cell Physiol*, 2018. 234(1): p. 23-32

<https://doi.org/10.1002/jcp.26865>.

10. Pickrell, A.M. and R.J. Youle, The roles of PINK1, parkin, and mitochondrial fidelity in Parkinson's disease. *Neuron*, 2015. 85(2): p. 257-73 <https://doi.org/10.1016/j.neuron.2014.12.007>.
11. Hou, X., J.O. Watzlawik, F.C. Fiesel, and W. Springer, Autophagy in Parkinson's Disease. *J Mol Biol*, 2020. 432(8): p. 2651-2672 <https://doi.org/10.1016/j.jmb.2020.01.037>.
12. Murakami, S., Y. Kusano, K. Okazaki, T. Akaike, and H. Motohashi, NRF2 signalling in cytoprotection and metabolism. *Br J Pharmacol*, 2023 <https://doi.org/10.1111/bph.16246>.
13. Li, J., C. Xu, and Q. Liu, Roles of NRF2 in DNA damage repair. *Cell Oncol (Dordr)*, 2023. 46(6): p. 1577-1593 <https://doi.org/10.1007/s13402-023-00834-5>.
14. George, M., M. Tharakan, J. Culberson, A.P. Reddy, and P.H. Reddy, Role of Nrf2 in aging, Alzheimer's and other neurodegenerative diseases. *Ageing Res Rev*, 2022. 82: p. 101756 <https://doi.org/10.1016/j.arr.2022.101756>.
15. Suzuki, T., J. Takahashi, and M. Yamamoto, Molecular Basis of the KEAP1-NRF2 Signaling Pathway. *Mol Cells*, 2023. 46(3): p. 133-141 <https://doi.org/10.14348/molcells.2023.0028>.
16. Ulasov, A.V., A.A. Rosenkranz, G.P. Georgiev, and A.S. Sobolev, Nrf2/Keap1/ARE signaling: Towards specific regulation. *Life Sci*, 2022. 291: p. 120111 <https://doi.org/10.1016/j.lfs.2021.120111>.
17. Zhang, W., C. Feng, and H. Jiang, Novel target for treating Alzheimer's Diseases: Crosstalk between the Nrf2 pathway and autophagy. *Ageing Res Rev*, 2021. 65: p. 101207 <https://doi.org/10.1016/j.arr.2020.101207>.
18. Brandes, M.S., J.A. Zweig, A. Tang, and N.E. Gray, NRF2 Activation Ameliorates Oxidative Stress and Improves Mitochondrial Function and Synaptic Plasticity, and in A53T α -Synuclein Hippocampal Neurons. *Antioxidants (Basel)*, 2021. 11(1) <https://doi.org/10.3390/antiox11010026>.
19. Jiang, T., B. Harder, M. Rojo de la Vega, P.K. Wong, E. Chapman, and D.D. Zhang, p62 links autophagy and Nrf2 signaling. *Free Radic Biol Med*, 2015. 88(Pt B): p. 199-204 <https://doi.org/10.1016/j.freeradbiomed.2015.06.014>.
20. Komatsu, M., p62 bodies: Phase separation, NRF2 activation, and selective autophagic degradation. *IUBMB Life*, 2022. 74(12): p. 1200-1208 <https://doi.org/10.1002/iub.2689>.
21. Veenstra, J.P. and J.J. Johnson, Rosemary (*Salvia rosmarinus*): Health-promoting benefits and food preservative properties. *Int J Nutr*, 2021. 6(4): p. 1-10.
22. Satoh, T., D. Trudler, C.K. Oh, and S.A. Lipton, Potential Therapeutic Use of the Rosemary Diterpene Carnosic Acid for Alzheimer's Disease, Parkinson's Disease, and Long-COVID through NRF2 Activation to Counteract the NLRP3 Inflammasome. *Antioxidants (Basel)*, 2022. 11(1) <https://doi.org/10.3390/antiox11010124>.
23. Ahmed, H.M. and M. Babakir-Mina, Investigation of rosemary herbal extracts (*Rosmarinus officinalis*) and their potential effects on immunity. *Phytother Res*, 2020. 34(8): p. 1829-1837 <https://doi.org/10.1002/ptr.6648>.
24. Ghasemzadeh Rahbardar, M. and H. Hosseinzadeh, Therapeutic effects of rosemary (*Rosmarinus officinalis* L.) and its active constituents on nervous system disorders. *Iran J Basic Med Sci*, 2020. 23(9): p. 1100-1112 <https://doi.org/10.22038/ijbms.2020.45269.10541>.
25. Chen, X.L., Q.Y. Luo, W.Y. Hu, J.J. Chen, and R.P. Zhang, Abietane Diterpenoids with Antioxidative Damage Activity from *Rosmarinus officinalis*. *J Agric Food Chem*, 2020. 68(20): p. 5631-5640 <https://doi.org/10.1021/acs.jafc.0c01347>.

26. Chen, X., Q. Luo, W. Hu, J. Chen, and R. Zhang, Labdane and isopimarane diterpenoids from *Rosmarinus officinalis* solid wastes: MS/MS spectrometric fragmentations and neuroprotective effect. *Industrial Crops and Products*, 2022. 177: p. 114441 <https://doi.org/10.1016/j.indcrop.2021.114441>.
27. Dovonou, A., C. Bolduc, V. Soto Linan, C. Gora, M.R. Peralta Iii, and M. Lévesque, Animal models of Parkinson's disease: bridging the gap between disease hallmarks and research questions. *Transl Neurodegener*, 2023. 12(1): p. 36 <https://doi.org/10.1186/s40035-023-00368-8>.
28. Yasuda, D., T. Ohe, K. Takahashi, R. Imamura, H. Kojima, T. Okabe, Y. Ichimura, M. Komatsu, M. Yamamoto, T. Nagano, and T. Mashino, Inhibitors of the protein-protein interaction between phosphorylated p62 and Keap1 attenuate chemoresistance in a human hepatocellular carcinoma cell line. *Free Radic Res*, 2020. 54(11-12): p. 859-871 <https://doi.org/10.1080/10715762.2020.1732955>.
29. Wang, Z., M. Yao, L. Jiang, L. Wang, Y. Yang, Q. Wang, X. Qian, Y. Zhao, and J. Qian, Dexmedetomidine attenuates myocardial ischemia/reperfusion-induced ferroptosis via AMPK/GSK-3 β /Nrf2 axis. *Biomed Pharmacother*, 2022. 154: p. 113572 <https://doi.org/10.1016/j.biopha.2022.113572>.
30. Luo, X., X. Weng, X. Bao, X. Bai, Y. Lv, S. Zhang, Y. Chen, C. Zhao, M. Zeng, J. Huang, B. Xu, T.W. Johnson, S.J. White, J. Li, H. Jia, and B. Yu, A novel anti-atherosclerotic mechanism of quercetin: Competitive binding to KEAP1 via Arg483 to inhibit macrophage pyroptosis. *Redox Biol*, 2022. 57: p. 102511 <https://doi.org/10.1016/j.redox.2022.102511>.
31. Marsh, J.M., S. Whitaker, L. Li, R. Fang, M.S.J. Simmonds, N. Vagkidis, and V. Chechik, The key phytochemistry of rosemary (*Salvia rosmarinus*) contributing to hair protection against UV. *Int J Cosmet Sci*, 2023. 45(6): p. 749-760 <https://doi.org/10.1111/ics.12883>.
32. Veenstra, J.P., B. Vemu, R. Tocmo, M.C. Nauman, and J.J. Johnson, Pharmacokinetic Analysis of Carnosic Acid and Carnosol in Standardized Rosemary Extract and the Effect on the Disease Activity Index of DSS-Induced Colitis. *Nutrients*, 2021. 13(3) <https://doi.org/10.3390/nu13030773>.
33. Hasei, S., T. Yamamotoya, Y. Nakatsu, Y. Ohata, S. Itoga, Y. Nonaka, Y. Matsunaga, H. Sakoda, M. Fujishiro, A. Kushiyama, and T. Asano, Carnosic Acid and Carnosol Activate AMPK, Suppress Expressions of Gluconeogenic and Lipogenic Genes, and Inhibit Proliferation of HepG2 Cells. *Int J Mol Sci*, 2021. 22(8) <https://doi.org/10.3390/ijms22084040>.
34. Lin, G., N. Li, D. Li, L. Chen, H. Deng, S. Wang, J. Tang, and W. Ouyang, Carnosic acid inhibits NLRP3 inflammasome activation by targeting both priming and assembly steps. *Int Immunopharmacol*, 2023. 116: p. 109819 <https://doi.org/10.1016/j.intimp.2023.109819>.
35. Bao, T.Q., Y. Li, C. Qu, Z.G. Zheng, H. Yang, and P. Li, Antidiabetic Effects and Mechanisms of Rosemary (*Rosmarinus officinalis* L.) and its Phenolic Components. *Am J Chin Med*, 2020. 48(6): p. 1353-1368 <https://doi.org/10.1142/s0192415x20500664>.
36. Warnecke, T., C. Lummer, J.W. Rey, I. Claus, and D. Lüttje, [Parkinson's disease]. *Inn Med (Heidelb)*, 2023. 64(2): p. 131-138 <https://doi.org/10.1007/s00108-022-01444-3>.
37. Nagatsu, T., A. Nakashima, H. Watanabe, S. Ito, and K. Wakamatsu, Neuromelanin in Parkinson's Disease: Tyrosine Hydroxylase and Tyrosinase. *Int J Mol Sci*, 2022. 23(8) <https://doi.org/10.3390/ijms23084176>.
38. Kawahata, I. and K. Fukunaga, Degradation of Tyrosine Hydroxylase by the Ubiquitin-Proteasome System in the Pathogenesis of Parkinson's Disease and Dopa-Responsive Dystonia. *Int J Mol Sci*, 2020. 21(11) <https://doi.org/10.3390/ijms21113779>.
39. Huang, T.I. and C.L. Hsieh, Effects of Acupuncture on Oxidative Stress Amelioration via Nrf2/ARE-Related Pathways in Alzheimer and Parkinson Diseases. *Evid Based Complement Alternat Med*, 2021. 2021: p. 6624976 <https://doi.org/10.1155/2021/6624976>.

40. Thiruvengadam, M., B. Venkidasamy, U. Subramanian, R. Samynathan, M. Ali Shariati, M. Rebezov, S. Girish, S. Thangavel, A.R. Dhanapal, N. Fedoseeva, J. Lee, and I.M. Chung, Bioactive Compounds in Oxidative Stress-Mediated Diseases: Targeting the NRF2/ARE Signaling Pathway and Epigenetic Regulation. *Antioxidants (Basel)*, 2021. 10(12) <https://doi.org/10.3390/antiox10121859>.
41. Villavicencio Tejo, F. and R.A. Quintanilla, Contribution of the Nrf2 Pathway on Oxidative Damage and Mitochondrial Failure in Parkinson and Alzheimer's Disease. *Antioxidants (Basel)*, 2021. 10(7) <https://doi.org/10.3390/antiox10071069>.
42. Malpartida, A.B., M. Williamson, D.P. Narendra, R. Wade-Martins, and B.J. Ryan, Mitochondrial Dysfunction and Mitophagy in Parkinson's Disease: From Mechanism to Therapy. *Trends Biochem Sci*, 2021. 46(4): p. 329-343 <https://doi.org/10.1016/j.tibs.2020.11.007>.
43. Eldeeb, M.A., R.A. Thomas, M.A. Ragheb, A. Fallahi, and E.A. Fon, Mitochondrial quality control in health and in Parkinson's disease. *Physiol Rev*, 2022. 102(4): p. 1721-1755 <https://doi.org/10.1152/physrev.00041.2021>.
44. Lizama, B.N. and C.T. Chu, Neuronal autophagy and mitophagy in Parkinson's disease. *Mol Aspects Med*, 2021. 82: p. 100972 <https://doi.org/10.1016/j.mam.2021.100972>.
45. Themistokleous, C., E. Bagnoli, R. Parulekar, and M.M.K. Muqit, Role of Autophagy Pathway in Parkinson's Disease and Related Genetic Neurological Disorders. *J Mol Biol*, 2023. 435(12): p. 168144 <https://doi.org/10.1016/j.jmb.2023.168144>.

